

1 **Dissolved organic carbon (DOC) in Arctic ground ice**

2

3 **M. Fritz¹, T. Opel¹, G. Tanski¹, U. Herzschuh^{1,2}, H. Meyer¹, A. Eulenburg¹ and H.**
4 **Lantuit^{1,2}**

5

6 [1] {Alfred Wegener Institute Helmholtz Centre for Polar and Marine Research, Department
7 of Periglacial Research, Potsdam, Germany}

8 [2] {University of Potsdam, Institute of Earth and Environmental Sciences, Potsdam,
9 Germany}

10

11 Correspondence to: M. Fritz (Michael.Fritz@awi.de)

12

1 **Abstract**

2 Thermal permafrost degradation and coastal erosion in the Arctic remobilize
3 substantial amounts of organic carbon (OC) and nutrients which have been accumulated in
4 late Pleistocene and Holocene unconsolidated deposits. Permafrost vulnerability to thaw
5 subsidence, collapsing coastlines and irreversible landscape change is largely due to the
6 presence of large amounts of massive ground ice such as ice wedges. However, ground ice
7 has not, until now, been considered to be a source of dissolved organic carbon (DOC),
8 dissolved inorganic carbon (DIC) and other elements, which are important for ecosystems and
9 carbon cycling. Here we show, using biogeochemical data from a large number of different
10 ice bodies throughout the Arctic, that ice wedges have the greatest potential for DOC storage
11 with a maximum of 28.6 mg L⁻¹ (mean: 9.6 mg L⁻¹). Variation in DOC concentration is
12 positively correlated with and explained by the concentrations and relative amounts of
13 typically terrestrial cations such as Mg²⁺ and K⁺. DOC sequestration into ground ice was more
14 effective during the late Pleistocene than during the Holocene, which can be explained by
15 rapid sediment and OC accumulation, the prevalence of more easily degradable vegetation
16 and immediate incorporation into permafrost. We assume that pristine snowmelt is able to
17 leach considerable amounts of well-preserved and highly bioavailable DOC as well as other
18 elements from surface sediments, which are rapidly frozen and stored in ground ice,
19 especially in ice wedges, even before further degradation. We found that ice wedges in the
20 Yedoma region represent a significant DOC (45.2 Tg) and DIC (33.6 Tg) pool in permafrost
21 areas and a fresh-water reservoir of 4,200 km³. This study underlines the need to discriminate
22 between particulate OC and DOC to assess the availability and vulnerability of the permafrost
23 carbon pool for ecosystems and climate feedback upon mobilization.

24

1 **1 Introduction**

2 Vast parts of the coastal lowlands of Siberia, Alaska and Canada consist of
3 unconsolidated organic-rich fine-grained deposits. These sediments, that occur as glacial
4 and Yedoma-type sediments (including their degradation forms as thermokarst), are
5 characterized by high ground-ice contents, both on a volumetric (vol%) and gravimetric
6 (weight %) basis (Brown et al., 1997; Zhang et al., 1999; Grosse et al., 2013; Schirmer et
7 al., 2013). Yedoma deposits, which formed during the late Pleistocene cold stages in
8 unglaciated Beringia (Schirmer et al., 2013), for instance, are characterized by absolute
9 ground-ice contents, excluding ice wedges, of 40-60 weight % (Schirmer et al., 2011c).
10 Ice wedges are one of the most common types of ground ice in permafrost. They form when
11 thermal contraction cracks open in winter, which are periodically filled with snow meltwater
12 in spring that quickly (re)freezes at negative ground temperatures to form ice veins and finally
13 vertically foliated ice wedges. The ice wedges are themselves characterized by volumetric ice
14 contents closing 100 vol% and make much of the subsurface in these Yedoma deposits.
15 Recent calculations of ice-wedge volumes in East Siberian Pleistocene Yedoma and Holocene
16 thermokarst deposits show contents of 48 vol% and 7 vol%, respectively (Strauss et al.,
17 2013). Combining ice wedges and other ice types in Yedoma deposits gives a mean
18 volumetric ground-ice content for those regions between 60 and 82 vol% (Zimov et al.
19 2006a, b; Schirmer et al., 2011b, c; Strauss et al., 2013). High ground-ice contents are
20 also typical for coastal Alaska (43-89 vol%; Kanevskiy et al., 2011, 2013) and the western
21 Canadian Arctic (50-60 vol%; French, 1998). The presence of massive ice (i.e. gravimetric ice
22 content >250% on dry soil weight basis; cf. van Everdingen, 1998) and excess ice, which is
23 visible ice that exceeds the pore space, is the key factor for the vulnerability of permafrost to
24 warmer temperatures and mechanical disturbance, as ice melt will initiate surface subsidence
25 and thermal collapse, also known as thermokarst (Czudek and Demek, 1970).
26 Permafrost soils hold approximately 50% of the global soil carbon pool (Tarnocai et al., 2009;
27 Hugelius et al., 2014), mostly as particulate organic carbon (POC). These calculations of
28 permafrost OC stocks, however, subtract the ground-ice content (Zimov et al. 2006a, b;
29 Tarnocai et al. 2009; Strauss et al., 2013; Hugelius et al., 2013, 2014) and therefore disregard
30 the OC, especially the amount of dissolved organic carbon (DOC), contained in large ground-
31 ice bodies such as ice wedges and other types of massive ice. Although these numbers might
32 be small compared to the POC stocks in peat and mineral soils, DOC from permafrost is
33 chemically labile (Dou et al., 2008; Vonk et al., 2013a, b) and may directly enter local food

1 webs. Due to its lability, DOC can become quickly mineralized by microbial communities
2 and photochemical reactions (Battin et al., 2008; Vonk et al., 2013a, b; Cory et al., 2014) and
3 returned to the atmosphere when released due to permafrost degradation (Schuur et al., 2009;
4 Schuur and Abbot, 2011).

5 Several studies have shed light on the POC stocks contained in permafrost (e.g. Zimov et al.,
6 2006a; Tarnocai et al., 2009; Schirrmeister et al., 2011b; Strauss et al., 2013; Hugelius et al.,
7 2013, 2014; Walter Anthony et al., 2014) and how much of these stocks is potentially
8 mobilized due to thermal permafrost degradation and coastal erosion (Rachold et al., 2004;
9 Jorgenson and Brown, 2005; Lantuit et al., 2009; McGuire et al., 2009; Ping et al., 2011;
10 Schneider von Deimling et al., 2012; Vonk et al., 2012; Günther et al., 2013; 2015; Wegner et
11 al., in review). DOC fluxes have also been quantified in western Siberian catchments (Frey
12 and Smith, 2005) and monitoring efforts of the large rivers draining permafrost areas and
13 entering into the Arctic Ocean have provided robust estimations of the riverine DOC export
14 (Raymond et al., 2007; McGuire et al., 2009). However, DOC stocks in permafrost ground ice
15 and the resulting potential DOC fluxes in response to coastal erosion and thermal degradation
16 are still unknown (Guo et al., 2007; Duo et al., 2008). At this moment, any inference about
17 DOC stocks in permafrost and fluxes from permafrost is derived from measurements in
18 secondary systems such as lake (e.g. Kling et al., 1991; Walter Anthony et al., 2014), river
19 (e.g. Benner et al., 2004; Finlay et al., 2006; Guo et al., 2007; Raymond et al., 2007; Holmes
20 et al., 2012) and ocean waters (e.g. Opsahl and Benner, 1997; Dittmar and Kattner, 2003;
21 Cooper et al., 2005) or from laboratory experiments (Dou et al., 2008). In contrast, the
22 purpose of this study was to sample and measure DOC at the source (i.e. ground ice in
23 permafrost) directly, before it gets altered by natural processes such as exposition to the
24 atmosphere, lithosphere and hydrosphere.

25
26 Here, we present an Arctic-wide study on DOC stocks in ground ice, aiming at incorporating
27 massive ground ice into the Arctic permafrost carbon budget. The specific objectives of our
28 study are:

- 29 • to quantify DOC contents in different massive ground ice types,
- 30 • to calculate DOC stocks in massive ground ice at the Arctic level,
- 31 • to put ground-ice-related DOC stocks into the context of the terrestrial Arctic OC
- 32 pools and fluxes, and

- 1
 - 2
 - 3
 - 4
 - 5
- to introduce relationships between organic and inorganic geochemical parameters, stable water isotopes, stratigraphy, and genetic and spatial characteristics to shed light on the origin of DOC and the processes of carbon sequestration in ground ice.

2 Study area and study sites

This study was carried out along the coastal lowlands of east Siberia, Alaska and northwest Canada (Fig. 1). All study sites, except for the Fairbanks area, are located within the zone of continuous permafrost. The sites cover a wide and representative range of geomorphological settings, terrain units and ground-ice conditions (Table 1). All studied ground-ice bodies were found in ice-rich unconsolidated Holocene and late Pleistocene (Marine isotope stages 2-5) deposits. Outcrops in permafrost were either accessible due to strong rates of coastal erosion along the ice-rich coasts forming steep exposures (Forbes, 2011) or were technically constructed for research purposes such as the CRREL Permafrost Tunnel in Barrow or for mining such as the Vault Creek Tunnel near Fairbanks, Alaska. Coastal outcrops in Siberia were dominated by large late Pleistocene ice wedges reaching up to 20 m in depth and up to 6 m in width (Schirrneister et al., 2011c). They formed syngenetically during periods of rapid sedimentation of Ice Complex deposits, also known as Yedoma (Schirrneister et al., 2013). Holocene epigenetic and syngenetic ice wedges of 1 – 6 m in depth and <1.0 – 3.5 m in width were encountered in exposed thermokarst depressions of Lateglacial¹ to Holocene origin and within the Holocene peaty cover deposits. Besides ice wedges, other types of massive ground ice were sampled, such as buried glacier ice, buried lake ice and a fossil snow patch (Fig. 2). In some cases, massive ground ice occupied as much as 90 vol% of 40 m coastal exposures eroding up to 10 m a⁻¹ (Lantuit et al., 2012). The focus of this paper is on massive ground ice; non-massive ice (in particular pore ice and intrasedimental ice such as ice lenses) was excluded from this first attempt to calculate DOC stocks in ground ice, because of the complex genetic processes associated with the interaction with enclosing sediment and the relatively small amount of ice relative to massive ice bodies. DOC in intrasedimental ice is, however, not considered to be insignificant.

¹ We refer to the Lateglacial as a stratigraphic and geochronological period at the transition between the Pleistocene and the Holocene. The Lateglacial spans the latest part of the Late Weichselian / Late Wisconsin glacial period. It includes the Bølling, the Older Dryas, the Allerød, and the Younger Dryas, from ca. 14,700 to 11,600 years before present (cf. de Klerk, 2004).

1 **3 Material and methods**

2 **3.1 Laboratory analyses**

3 A total number of 101 ice samples from 29 ice bodies and 3 surface water samples
4 from 3 thermokarst lakes were studied. Ice blocks were cut with a chain saw in the field and
5 kept frozen until further processing with a band saw in a cold lab at -15°C for removal of
6 partially melted margins and cleaning of the edges. Samples ≥ 50 ml were thawed at 4°C in
7 pre-cleaned (purified water) glass beakers covered with pre-combusted aluminium foil
8 (550°C). Meltwater was filtered with gum-free syringes equipped with glass fibre filters
9 (WhatmanTM GF/F; pore size: $0.7\ \mu\text{m}$) and acidified with $20\ \mu\text{l}$ $\text{HCl}_{\text{suprapur}}$ (30%) to $\text{pH} < 2$ in
10 order to prevent microbial conversion. DOC concentrations (mg L^{-1}) were measured with a
11 high-temperature (680°C) combustion total organic carbon analyzer (Shimadzu TOC-V_{CPH}).
12 Internal acidification is used to convert inorganic carbon into CO_2 , which is stripped out of
13 solution. Non-purgeable organic carbon compounds are combusted and converted to CO_2 and
14 measured by a non-dispersive infrared detector (NDIR). The device-specific detection limit is
15 $0.4\ \mu\text{g L}^{-1}$. For each sample, one measurement with three to five repetitions was performed
16 and results were averaged.

17 Further analyses for hydrochemical characterization included pH, electrical conductivity,
18 major anions and cations, and stable water isotopes ($\delta^{18}\text{O}$, δD). Stratigraphic investigations
19 and stable water isotopes were used to differentiate between genetic ice types and to assess
20 their approximate age (i.e. Holocene and late Pleistocene). Analyses of $\delta^{18}\text{O}$ and δD were
21 carried out with a mass spectrometer (Finnigan MAT Delta-S) using the water-gas
22 equilibration technique (for further information see [Horita et al., 1989](#); [Meyer et al., 2000](#)).
23 The isotopic composition is expressed in delta per mil notation (δ , ‰) relative to the Vienna
24 Standard Mean Ocean Water (VSMOW) standard. The reproducibility derived from long-
25 term standard measurements is established with 1σ better than ± 0.1 ‰ for $\delta^{18}\text{O}$ and ± 0.8 ‰
26 for δD ([Meyer et al., 2000](#)). Samples for ion analysis were passed through cellulose-acetate
27 filters (WhatmanTM CA; pore size $0.45\ \mu\text{m}$). Afterwards, samples for the cation analyses were
28 acidified with $\text{HNO}_3_{\text{suprapur}}$ (65%) to prevent microbial conversion processes and adsorptive
29 accretion, whereas samples for anion analyses were kept cool. The cation content was
30 analysed by Inductively Coupled Plasma-Optical Emission Spectrometry (ICP-OES, Perkin-
31 Elmer Optima 3000 XL), while the anion content was determined by Ion Chromatography
32 (IC, Dionex DX-320). Hydrogen carbonate concentrations were measured by titration with

1 0.01 M HCl using an automatic titrator (Metrohm 794 Basic Titrino). Based on HCO_3^-
2 concentrations we approximated the dissolved inorganic carbon (DIC) concentrations using
3 the molecular weights.
4

5 **3.2 Statistical methods**

6 **3.2.1 Principal Component Analysis (PCA)**

7 Principal component analysis (PCA) was used to summarize the variation in a biplot
8 by reducing dimensionality of the data while retaining most of the variation in the data set
9 (Jolliffe, 2002). Ordinally scaled variables (i.e. chemical data set) were log-transformed,
10 centered and standardized except for pH, $\delta^{18}\text{O}$, δD , latitude, and longitude not being log-
11 transformed due the inter-sample invariance. Ice types (ice wedge, buried lake ice, basal
12 glacier ice, snow pack ice, surface water), relative age (Pleistocene, Holocene, recent) were
13 coded with dummy variables and were superimposed as inactive supplementary variables on
14 the ordination plot to enable rough assumptions about the relationship between chemical
15 composition, ground-ice formation and age. The whole data set was reduced to 92 samples
16 and 23 variables by removing those containing missing values. PCA was performed with
17 focusing on inter-species correlation and was implemented using CANOCO 4.5 software for
18 Windows (ter Braak and Šmilauer, 2002).
19

20 **3.2.2 Univariate Tree Models (UTM)**

21 A powerful tool to explore the relationship between a single continuous response
22 variable (DOC concentration) and multiple explanatory variables is a regression tree (Zuur et
23 al., 2007). Tree models perform well with non-linearity and interaction between explanatory
24 variables. UTM is used to find interactions missed by other methods and also indicate the
25 relative importance of different explanatory variables. UTM was performed using the
26 computing environment R and Brodgar 2.6.5 software for Windows (ter Braak and Šmilauer,
27 2002).
28

1 4 Results

2 4.1 DOC and DIC concentrations

3 [Table 2](#) provides an overview of mean DOC and DIC concentrations and range for
4 each ground-ice type. We found strong variations of DOC concentrations within and across
5 individual ground-ice types. The highest DOC concentrations were found in ice wedges with
6 a mean of 9.6 mg L⁻¹ and a maximum of 28.6 mg L⁻¹. Late Pleistocene ice wedges were
7 characterized by higher mean DOC concentrations than Holocene ones with 11.1 and
8 7.3 mg L⁻¹, respectively. Other ice types had average DOC concentrations between 1.8 and
9 3.0 mg L⁻¹ and their range was narrower than in ice wedges ([Table 2](#), [Fig. 3](#)). Modern surface
10 water gave DOC values between 5.5 and 5.8 mg L⁻¹.

11 The highest DIC concentrations were found in modern surface water with on average
12 22.6 mg L⁻¹ and a maximum of 40.2 mg L⁻¹ ([Table 2](#), [Fig. 3](#)). DIC concentrations were lower
13 in ground ice but varied strongly across ice types. With 8.5 mg L⁻¹ late Pleistocene ice wedges
14 were characterized by almost four times higher mean DIC concentrations than Holocene ones
15 (2.2 mg L⁻¹; [Fig. 3](#)). Buried glacier and lake ice had similar mean DIC concentrations (around
16 9 mg L⁻¹) but showed large ranges; from values around zero up to 25 mg L⁻¹. Basal glacier
17 ice, buried lake ice, and snow pack ice show mean DOC concentrations between 1.8 and
18 3.0 mg L⁻¹. For individual sample values see [Supplement Table S1](#).

19

20 4.2 Correlation matrix

21 With the help of a correlation matrix environmental processes and chemical
22 relationships can be visualized that may help to explain the sequestration of DOC into ground
23 ice. Pearson's correlation coefficients were calculated and plotted in a correlation matrix in
24 order to assess the degree of association between DOC, chemical properties, stable water
25 isotopes and spatial variables ([Fig. 4](#)). A strong positive correlation suggests a mutual driving
26 mechanism whereas negative values imply an inverse association. Most importantly, DOC is
27 positively related to the relative proportion of Mg²⁺ in the cation spectrum (R=0.65). Further
28 positive relations between DOC and other parameters, although less pronounced, involve K⁺
29 (R=0.36), HCO₃⁻ (R=0.36) and latitude (R=0.38). The only significantly negative relationship

1 with regard to DOC exists together with Na^+ ($R=-0.44$) (Fig. 4). Climate-driven parameters
2 such as $\delta^{18}\text{O}$, δD , and D-excess do not explain DOC concentrations.

3

4 **4.3 Principal components**

5 The first two axes of the PCA explain 43.9% of the variation in the data (Fig. 5). Cl^-
6 and Na^+ ions are positively correlated with the first axis in descending order of correlation,
7 whereas Ca^{2+} , Mg^{2+} , and HCO_3^- ions and pH are negatively correlated. Parameters positively
8 correlated with PCA axis 2 include information on the ice origin as Pleistocene and basal
9 glacier ice. In contrast, δD , $\delta^{18}\text{O}$, DOC concentration, and information on the ice origin as ice
10 wedge and Holocene ground ice are negatively correlated with PCA axis 2. Variations in
11 SO_4^{2-} and NO_3^- concentration as well as information on latitude and longitude are not
12 correlated with the first two PCA axes. The separation of ice samples in the PCA ordination
13 plot leads to three distinct groups: (1) Holocene ice wedges and recent surface water samples
14 are entirely negatively related to the second axis, whereas (2) Pleistocene ice wedges are
15 entirely negatively related to the first axis. (3) Pleistocene basal glacier ice and buried lake ice
16 is positively related to the second axis. This separation might be related to the different
17 processes of ice formation and climate variation.

18 Na^+ and Cl^- -dominated samples represent Holocene ice wedges from coastal cliffs in east
19 Siberia (Muostakh Island and Oyogos Yar). The majority of ice wedges with a terrestrial ion
20 composition (Mg^{2+} , Ca^{2+} , HCO_3^-) are of late Pleistocene age in areas such as Mamontov Klyk,
21 Bol'shoy Lyakhovsky Island, Yukon Coast and the Fairbanks area. The first axis probably
22 separates samples with a strong marine impact at its upper end from those with more of a
23 continental background. The second axis might represent climate conditions of formation.
24 The majority of Pleistocene ice samples with a depleted stable water isotope composition
25 show positive sample scores whereas Holocene ground ice being enriched in heavy stable
26 water isotopes mostly shows negative sample scores and therefore plots in the lower part of
27 the PCA (Fig. 5).

28

1 **4.4 Univariate Tree Model (UTM)**

2 UTM (Fig. 6a) shows that differences in DOC concentrations can be explained according to
3 inorganic geochemical properties. The first two nodes split on Mg^{2+} with a threshold value of
4 16% of the cation spectrum. The next nodes split according to thresholds in K^+ of 2.30 and
5 2.65%, respectively (Fig. 6a). Threshold percentages presented here are based on the cation
6 spectrum only. This means that all measured cations sum up to 100 %. This is statistically
7 more robust than using individual sample concentrations which can have different
8 magnitudes. We end up with four statistically significant groups (i.e. nodes) with different
9 mean DOC concentrations ($mg\ L^{-1}$) of each group, also showing the number of observations
10 in each group (n). With the UTM information – that inorganic geochemistry explains the
11 variability in DOC concentration – we can make assumptions about relations between carbon
12 sequestration in different water types. DOC concentration is not independent from inorganic
13 geochemical composition. Cross validation (Fig. 6b) confirms statistical significance of the
14 model result.

15

16

5 Discussion

5.1 DOC stocks in ground ice and relevance to carbon cycling

While the riverine DOC export to the Arctic Ocean has been estimated to 33-34 Tg a⁻¹ (McGuire et al. 2009; Holmes et al., 2012), comparable numbers for the DOC input by coastal erosion and thermal permafrost degradation (also known as thermokarst) are not available yet. This knowledge gap includes the DOC contribution derived from melting ground ice from ice-rich permafrost. Table 2 provides an overview of DOC contents in different massive ground-ice types from the North American and Siberian Arctic. Because of their wide spatial distribution in Arctic lowlands and the measured DOC concentrations, we conclude that from massive ground-ice types ice wedges hold the greatest potential for DOC storage with a maximum of 28.6 mg L⁻¹. This is in good agreement with DOC measurements in a so far limited number of ice wedges by Douglas et al. (2011) in Alaska and Vonk et al. (2013b) in east Siberia who showed DOC concentrations of 18.4 – 68.5 mg L⁻¹ (n=5) and 8.8 – 15 mg L⁻¹ (n=3), respectively.

Ulrich et al., (2014) have calculated maximum wedge ice volumes (WIV), which range from 31.4 to 63.2 vol% for late Pleistocene Yedoma deposits and from 6.6 to 13.2 vol% for Holocene thermokarst deposits in east Siberia and Alaska. Strauss et al. (2013) have shown similar averages for WIV of 48 vol% in late Pleistocene Yedoma and 7.0 vol% for Holocene thermokarst deposits. Together with average DOC concentrations of 11.1 mg L⁻¹ (max. 28.6) this would lead to 5.3 g DOC per m³ (max. 18.1) for late Pleistocene ice wedges in the upper late Pleistocene permafrost column (Table 3) and a DOC pool of 43.0 Tg DOC based on 416,000 km² of undisturbed Yedoma in Beringia and a mean thickness of 19.4 m (Strauss et al., 2013). DOC stocks in ice wedges in Holocene thermokarst deposits are much lower with on average 0.51 g m⁻³ and a maximum of 2.6 g m⁻³ due to much lower WIV (cf. Ulrich et al., 2014) and slightly lower DOC concentrations (Table 3). With on average 2.2 Tg the Holocene ice wedge DOC pool is much lower than the late Pleistocene pool, mainly because of lower WIV, an average thickness of 5.5 m for thermokarst deposits and despite their greater extent (775,000 km²) than undegraded Yedoma deposits (Strauss et al., 2013). Even stronger differences are characteristic for DIC pools in late Pleistocene ice wedges (32.9 Tg) compared to Holocene ice wedges (0.66 Tg) in the same areas. Based on the above-mentioned spatial coverage of Yedoma and thermokarst deposits including sediment thickness and WIV, we

1 conclude that in the study area ice wedges represent a significant DOC (45.2 Tg) and DIC
2 (33.6 Tg) pool in permafrost areas and a fresh-water reservoir of 4,200 km³ (see [Table 3](#)).
3 However, all types of non-massive intrasedimental ice, raising the total ground-ice volume to
4 ~80% ([Schirrmeister et al., 2011b](#); [Strauss et al., 2013](#)), are still excluded. DOC
5 concentrations in non-massive intrasedimental ice from Muostakh Island (Siberia) and the
6 Yukon Coast (Canada) have been found to be much higher (Fritz, unpublished data). Higher
7 DOC concentrations in intrasedimental ice than in massive ice are certainly due to the long-
8 term contact of soil moisture with soil organic matter prior to freezing. We therefore suggest
9 that incorporating DOC from non-massive ground-ice types would lead to a significant rise in
10 DOC stocks in permafrost of at least one order of magnitude. However, a differentiation
11 between particulate and dissolved OC in permafrost is not done yet, although the technical
12 means via rhizon soil moisture sampling is already available on a cost- and time-efficient
13 basis. Nevertheless, we are aware of the fact that DOC makes up a limited proportion of the
14 whole permafrost carbon stocks. A cautious estimation of the ratio of DOC and POC is in the
15 order of ~1/2000 if we consider about 2 wt% total organic carbon (TOC) in sediments (e.g.
16 [Schirrmeister et al., 2011b,c](#); [Strauss et al., 2013](#)) and about 10 mg L⁻¹ DOC in massive ground
17 ice. This ratio will become much smaller if POC and DOC in the whole permafrost column
18 would be differentiated, because TOC comprises both POC and DOC.

19

20 **5.2 Carbon sequestration and origin in relation to inorganic geochemistry**

21 The origin and sequestration process into ground ice seems to play an important role in
22 the magnitude and bioavailability of DOC. Sequestration of OC into ground ice is a complex
23 process that is dependent on water source, freezing process, organic matter origin and
24 inorganic geochemical signature of the ambient water to form ground ice.

25 [Figures 4 and 6a](#) show that the electrical conductivity (i.e. total ion content) of ground ice is
26 unrelated to DOC but that the ion composition and therefore the ion source seems to be
27 relevant. Mg²⁺ and K⁺ are the most significant parameters for explaining variations in DOC
28 concentrations ([Fig. 6a](#)). Higher Mg²⁺ and K⁺ fractions of the cations spectrum are positively
29 related to higher DOC concentrations ([Fig. 4](#)). We recognize that in the node (group) with the
30 highest average DOC concentrations ($\bar{\varnothing} = 11.9 \text{ mg L}^{-1}$, n=40) we find most of the Pleistocene
31 ice wedges and to a lesser extent Holocene ice wedges ([Fig. 6a](#)). All study areas are
32 represented here. Both, Mg²⁺ and K⁺ have typically high shares in terrestrial water types

1 because Mg and K are major elements in clay minerals and feldspars. In combination with
2 terrestrial HCO_3^- and Ca^{2+} the mobility of Mg^{2+} is high in $\text{Mg}/\text{Ca}(\text{HCO}_3)_2$ solutions ([Granse](#)
3 [and Führs, 2013](#)).

4

5 Ice wedges are fed by meltwater from atmospheric sources that have been in contact with
6 vegetation and sediments of the tundra surface before meltwater infiltrated the frost cracks in
7 spring. By contrast, glacier ice, buried snow bank ice, and lake ice is primarily fed by
8 atmospheric waters having less interaction with carbon and ion sources. Yet, the yellowish
9 brown to gray late Pleistocene and the milky-white Holocene ice wedges have incorporated
10 sediments and organic matter that originates from surface soils and vegetation debris that was
11 carried along with the meltwater into the frost crack (e.g. [Opel et al., 2011](#)). Spring snow melt
12 water interacts with the soil material leaching out carbon as it trickles downward toward the
13 ice wedges. Also, since wedges may take thousands of years to form and the location of their
14 upper surface changes with time, there are numerous spatial and temporal ways that deeper
15 soil pore waters can get incorporated into the wedge ice. Leaching of DOC from relatively
16 young surface organic matter takes place ([Guo et al., 2007](#); [Lachniet et al., 2012](#)) as well as
17 dissolution of ions from sediment particles. Snow melt feeding ice wedges strongly attracts
18 leachable components because of its initial purity. This might be the reason why especially
19 ice wedges contain relatively high amounts of bioavailable DOC with low-molecular weight
20 compounds that can be old but remained fresh over millennia ([Vonk et al., 2013b](#)).

21

22 Principal component analysis clusters ice wedges into two main groups along the first axis
23 based on Na^+ and Cl^- dominating Holocene ice wedges in modern coastal settings and Mg^{2+} ,
24 Ca^{2+} and HCO_3^- for Pleistocene ice wedges and Holocene ones being far from coasts ([Fig. 5](#)).
25 This pattern depicts the competing influence of maritime and terrestrial/continental
26 conditions. A similar differentiation of ice wedges (and all ground ice types) is done along the
27 second PCA axis ([Fig. 5](#)). Differences in stable water isotopes indicate the predominant
28 climate variations between the late Pleistocene and the Holocene which are also reflected in
29 the landscape (i.e. distance to sea; maritime vs. continental). Distance from the coastline is
30 crucial for the incorporation of marine-derived ions through aerosols such as NaCl via sea
31 spray. While the Fairbanks area is the only site far inland, all other study sites except for
32 Samoylov Island in the central Lena River Delta are coastal areas today. However, during the
33 late Pleistocene global sea level was lower and large parts of the shallow circum-arctic

1 shelves were subaerially exposed. Present-day coastal sites were located up to hundreds of
2 kilometers inland. Marine ion transport via sea spray is not expected to have played a role on
3 inland sites but indeed since the rapid marine transgression during the Holocene that changed
4 far inland sites into coastal ones. Input of sea spray is only relevant during the open-water
5 season so that a prolonged ice cover during the late Pleistocene (Nørgaard-Pedersen et al.,
6 2003; Bradley and England, 2008) should have further reduced the influx of sea salt.
7 Additionally, sustained dry conditions (Carter, 1981; Alfimov and Berman, 2001; Murton,
8 2009) probably increased eolian input of terrestrial material into ice wedges which is then
9 directly mirrored in the hydrochemical signature.

10
11 So far we have shown that coastal/maritime and terrestrial environmental conditions can be
12 differentiated based on inorganic hydrochemistry and that terrestrial surface OC sources feed
13 the DOC signal in ice wedges. DOC sequestration into ground ice is also dependent on active
14 layer properties, vegetation cover, vegetation communities, and deposition rates. Long-term
15 stable surfaces and relatively constant active layer depths will lead to substantially leached
16 soil layers in terms of DOC (Guo and Macdonald, 2006) and inorganic solutes (Kokelj et al.,
17 2002). Based on $\Delta^{14}\text{C}$ values and $\delta^{13}\text{C}$ ratios on DOC from soil leaching experiments and
18 natural river water samples, Guo et al. (2007) have shown that intensive leaching of DOC
19 from young and fresh plant litter and upper soil horizons occurs during the snowmelt period.
20 Later in the season, DOC yields decreased in rivers draining permafrost areas, indicating that
21 deepening of the active layer and leaching of deeper seasonally frozen soil horizons were
22 accompanied by much lower concentrations of DOC due to the refractory and insoluble
23 character of the remaining organic matter compounds. In addition, dissolved organic matter
24 compounds in runoff into lakes and rivers can become rapidly degraded by microbial
25 communities and photochemical reactions (Striegl et al., 2005; Olefeldt and Roulet, 2012;
26 Cory et al., 2014). One destination of the fresh, young and therefore most bioavailable DOC
27 components will be ice wedges (Vonk et al., 2013b), where the chemical character is
28 preserved because of immediate freezing. This highlights the importance of ground ice and
29 especially ice wedges as a vital source of bioavailable DOC.

30

5.3 DOC mobility and quality upon permafrost degradation

The absolute numbers of DOC in permafrost might be still small compared to the POC. However, POC from both peat and mineral soil has a relatively slow decomposition rate after thaw compared to DOC (Schuur et al., 2008). Organic matter from melting ground ice was shown to be highly bioavailable and can even enhance organic matter degradation of the host material by increased enzyme activity in ice wedge meltwater (Vonk et al., 2013b). Bioavailability experiments with Yedoma DOC from thaw streams fed by ice wedge meltwater in NE Siberia illustrated the rapid decomposability of Yedoma OC, with OC losses of up to 33% in 14 days (Vonk et al. 2013a). Incubations with increasing amounts of ice wedge water in the Yedoma-water suspension enhanced DOC loss over time. Vonk et al. (2013b) concluded that ice wedges contain a DOM pool of reduced aromaticity and can be therefore regarded as an old but readily available carbon source with a high content of low-molecular weight compounds. Additionally, a co-metabolizing effect through high potential enzyme activity in ice wedges upon thaw leads to enhanced degradation rates of organic matter of the host material. When studying organic matter cycling in permafrost areas we have to abandon the paradigm, which holds true for temperate regions and Arctic oceanography, that old OC is refractory and that only young OC is fresh, bioavailable, and therefore relevant for food webs and greenhouse gas considerations.

We suggest that reduced organic matter degradation during cold periods is the main reason why late Pleistocene syngenetic ice wedges have incorporated more DOC on average than Holocene ice wedges. Incorporation of soluble organic matter into ground ice might have been more effective than today due to various reasons. Ice Complex deposits in the coastal lowlands formed during the late Pleistocene cold period, when high accumulation rates of fine-grained sediments and organic matter were accompanied by rapidly aggrading permafrost (Hubberten et al., 2004). This means that organic matter is less decomposed because it was rapidly incorporated into perennially frozen ground and into the surrounding syngenetic ice wedges as the permafrost table rose together with the rising surface during deposition (Schirmer et al., 2011b). Also, colder annual air temperatures led to reduced decomposition rates of organic matter which originated from vegetation communities dominated by easily decomposable forbs (Willerslev et al., 2014) in contrast to resistant sedge-moss-shrub tundra vegetation since postglacial times (Andreev et al., 2011). Additionally, low precipitation and reduced runoff presumably retained more DOC in the landscape, ready to be transported into frost cracks.

1
2
3
4
5
6
7
8
9
10
11
12
13
14
15
16
17
18
19
20
21
22
23
24
25
26
27
28
29
30
31
32

Guo et al. (2007) concluded that most of the DOC in Arctic rivers is derived from young and fresh plant litter and upper soil horizons. Leaching of deeper seasonally frozen soil horizons is accompanied by much lower DOC concentrations due to the refractory and insoluble character of the remaining organic matter compounds (Guo et al., 2007). DOC impoverishment in the active layer is logical as it is leached each season over a long time under modern climate conditions, where permafrost aggradation is much slower than during cold stages; if it happens at all. The quantity and quality of DOC pools in deeper permafrost is probably much higher because of – so far – suppressed remobilization. Dou et al. (2008) studied the production of DOC as water-extractable organic carbon (WEOC) yields from organic-rich soil horizons in the active layer and permafrost from a coastal bluff near Barrow (Alaska) facing the Beaufort Sea. Besides high DOC yields in the uppermost horizon (0-5 cm below surface) the second highest DOC yields derived from permafrost although the sampled horizon showed lower soil OC contents than others (Dou et al., 2008). Interestingly, higher fractions of low-molecular-weight DOC, which is regarded to be more bioavailable, were generally found at greater depths. This supports the view that permafrost deposits hold a great potential for mobilizing large quantities of highly bioavailable organic matter upon degradation. Coastal erosion and thermokarst often expose old and deep permafrost strata. Contained organic matter is directly exposed to the atmosphere and transferred into coastal and fresh-water ecosystems without degradation because of short travel and residence times. Therefore, Arctic coastal zones are supposed to receive high loads of bioavailable dissolved and particulate organic matter. Dou et al. (2008) used pure water (presumably MilliQ) and natural sea water as solvent for studying the production of DOC. It turned out that seawater extraction significantly reduced DOC yields which were attributed mainly to reduced solubility of humic substances due to the presence of polyvalent cations such as Ca^{2+} and Mg^{2+} in seawater (Aiken and Malcolm, 1987). On the one hand Dou et al. (2008) invoked that a laboratory setup using pure water and dried/rewetted soil samples would lead to an overestimation of DOC input to the Arctic Ocean during coastal erosion. On the other hand and based on the large ground-ice volumes in coastal cliffs (Lantuit et al., 2012), we suggest that ice wedge meltwater with a low ion content is probably able to leach greater amounts of DOC from permafrost upon thaw than other natural surface water.

1 An open question remains how much DOC can be found in intrasedimental ice and how much
2 DOC is produced upon degradation of old permafrost (e.g. late Pleistocene Yedoma type) for
3 example as a result of coastal erosion. The answer to this question is crucial to follow the fate
4 of permafrost organic matter upon re-mobilization. Additionally, robust estimations of carbon
5 release are crucial for predicting the strength and timing of carbon-cycle feedback effects, and
6 thus how important permafrost thaw will be for climate change this century and beyond.
7

6 Conclusions and outlook

Ground ice in ice-rich permafrost deposits contains DOC, DIC and other nutrients, which are relevant to the global carbon cycle, arctic fresh-water habitats and marine food webs upon release.

The following conclusions can be drawn from this study:

- Ice wedges represent a significant DOC (45.2 Tg) and DIC (33.6 Tg) pool in the studied permafrost areas and a considerable fresh-water reservoir of 4,200 km³.
- Syngenetic late Pleistocene ice wedges have the greatest potential to host a large pool of presumably bioavailable DOC because of i) highest measured average DOC concentrations in combination with ii) their wide spatial (lateral, vertical) distribution in ice-rich permafrost areas and iii) the sequestration of fresh and easily leachable OC compounds.
- Increased incorporation of DOC into ground ice is linked to relatively high proportions of terrestrial cations, especially Mg²⁺ and K⁺. This indicates that leaching of terrestrial organic matter is the most relevant process of DOC sequestration into ground ice.

Based on our results about the stocks and chemical behavior of DOC in massive ground-ice bodies we propose that further studies shall strive to:

- quantify DOC fluxes in the Arctic from thawing permafrost, melting ground ice and coastal erosion,
- differentiate between DOC and POC in permafrost including non-massive intrasedimental ice,
- quantify DOC production from permafrost in different stratigraphic settings and with different natural solvents to answer the question, what fraction of soil OC will be leached as DOC,
- assess the age and lability of DOC versus POC in permafrost and the potential impact on coastal food webs and fresh-water ecosystems.

1 **Acknowledgements**

2 We thank the Yukon Territorial Government, the Yukon Parks (Herschel Island
3 Qiqiktaruk Territorial Park), Parks Canada office (Ivvavik National Park) and the Aurora
4 Research Institute – Aurora College (ARI) in Inuvik, NWT, for administrative and logistical
5 support. This study was partly funded by the International Bureau of the German Federal
6 Ministry of Education and Research (grant no. CAN 09/001, 01DM12002 to H.L.), the
7 Helmholtz Association (grant no. VH-NG-801 to H.L.), the German Research Foundation
8 (grant no. OP217/2-1 to T.O.), and a fellowship to M.F. by the German Federal
9 Environmental Foundation (DBU). Analytical work at AWI received great help from Ute
10 Kuschel. Sebastian Wetterich, Dave Fox, and Stefanie Weege assisted in the field. We
11 acknowledge two anonymous reviewers and the editor Stephan Gruber for their helpful
12 comments and suggestions.

13

1 References

- 2 Aiken, G. R., and Malcolm, R. L.: Molecular weight of aquatic fulvic acids by vapor pressure
3 osmometry, *Geochimica et Cosmochimica Acta*, 51, 2177-2184, doi:10.1016/0016-
4 7037(87)90267-5, 1987.
- 5 Alfimov, A. V., and Berman, D. I.: Beringian climate during the Late Pleistocene and
6 Holocene, *Quaternary Science Reviews*, 20, 127-134, doi:10.1016/S0277-3791(00)00128-
7 1, 2001.
- 8 Andreev, A. A., Tarasov, P., Schwamborn, G., Ilyashuk, B., Ilyashuk, E., Bobrov, A.,
9 Klimanov, V., Rachold, V., and Hubberten, H.-W.: Holocene paleoenvironmental records
10 from Nikolay Lake, Lena River Delta, Arctic Russia, *Palaeogeography, Palaeoclimatology,*
11 *Palaeoecology*, 209, 197-217, doi:10.1016/j.palaeo.2004.02.010, 2004.
- 12 Andreev, A. A., Grosse, G., Schirrmeister, L., Kuznetsova, T. V., Kuzmina, S. A., Bobrov, A.
13 A., Tarasov, P. E., Novenko, E. Y., Meyer, H., Derevyagin, A. Y., Kienast, F., Bryantseva,
14 A., and Kunitsky, V. V.: Weichselian and Holocene palaeoenvironmental history of the
15 Bol'shoy Lyakhovsky Island, New Siberian Archipelago, Arctic Siberia, *Boreas*, 38, 72-
16 110, doi:10.1111/j.1502-3885.2008.00039.x, 2009.
- 17 Andreev, A. A., Schirrmeister, L., Tarasov, P. E., Ganopolski, A., Brovkin, V., Siegert, C.,
18 Wetterich, S., and Hubberten, H.-W.: Vegetation and climate history in the Laptev Sea
19 region (Arctic Siberia) during Late Quaternary inferred from pollen records, *Quaternary*
20 *Science Reviews*, 30, 2182-2199, doi:10.1016/j.quascirev.2010.12.026, 2011.
- 21 Battin, T. J., Kaplan, L. A., Findlay, S., Hopkinson, C. S., Marti, E., Packman, A. I.,
22 Newbold, J. D., and Sabater, F.: Biophysical controls on organic carbon fluxes in fluvial
23 networks, *Nature Geosci*, 1, 95-100, doi:10.1038/ngeo101, 2008.
- 24 Benner, R., Benitez-Nelson, B., Kaiser, K., and Amon, R. M. W.: Export of young
25 terrigenous dissolved organic carbon from rivers to the Arctic Ocean, *Geophys. Res. Lett.*,
26 31, L05305, doi:10.1029/2003gl019251, 2004.
- 27 Boereboom, T., Samyn, D., Meyer, H., and Tison, J. L.: Stable isotope and gas properties of
28 two climatically contrasting (Pleistocene and Holocene) ice wedges from Cape Mamontov
29 Klyk, Laptev Sea, northern Siberia, *The Cryosphere*, 7, 31-46, doi:10.5194/tc-7-31-2013,
30 2013.
- 31 Bradley, R. S., and England, J. H.: The Younger Dryas and the Sea of Ancient Ice,
32 *Quaternary Research*, 70, 1-10, doi:10.1016/j.yqres.2008.03.002, 2008.
- 33 Brown, J., O.J. Ferrians, Jr., J.A. Heginbottom, and E.S. Melnikov, eds. 1997. Circum-Arctic
34 map of permafrost and ground-ice conditions. Washington, DC: U.S. Geological Survey in
35 Cooperation with the Circum-Pacific Council for Energy and Mineral Resources. Circum-
36 Pacific Map Series CP-45, scale 1:10,000,000, 1 sheet.
- 37 Carter, L. D.: A Pleistocene sand sea on the Alaskan Arctic Coastal Plain, *Science*, 211, 381-
38 383, doi:10.1126/science.211.4480.381, 1981.
- 39 Cooper, L. W., Benner, R., McClelland, J. W., Peterson, B. J., Holmes, R. M., Raymond, P.
40 A., Hansell, D. A., Grebmeier, J. M., and Codispoti, L. A.: Linkages among runoff,

- 1 dissolved organic carbon, and the stable oxygen isotope composition of seawater and other
2 water mass indicators in the Arctic Ocean, *J. Geophys. Res.*, 110, G02013,
3 doi:10.1029/2005jg000031, 2005.
- 4 Cory, R. M., Ward, C. P., Crump, B. C., and Kling, G. W.: Sunlight controls water column
5 processing of carbon in arctic fresh waters, *Science*, 345, 925-928,
6 doi:10.1126/science.1253119, 2014.
- 7 Czudek, T. and Demek, J.: Thermokarst in Siberia and its influence on the development of
8 lowland relief, *Quaternary Research*, 1, 103-120, doi:10.1016/0033-5894(70)90013-X,
9 1970.
- 10 de Klerk, P.: Confusing concepts in Lateglacial stratigraphy and geochronology: origin,
11 consequences, conclusions (with special emphasis on the type locality Bøllingsø), *Review*
12 *of Palaeobotany and Palynology*, 129, 265-298, doi:10.1016/j.revpalbo.2004.02.006, 2004.
- 13 Dittmar, T., and Kattner, G.: The biogeochemistry of the river and shelf ecosystem of the
14 Arctic Ocean: a review, *Marine Chemistry*, 83, 103-120, doi:10.1016/S0304-
15 4203(03)00105-1, 2003.
- 16 Dou, F., Ping, C.-L., Guo, L., and Jorgenson, T.: Estimating the impact of seawater on the
17 production of soil water-extractable organic carbon during coastal erosion, *Journal of*
18 *Environmental Quality*, 37, 2368-2374, doi:10.2134/jeq2007.0403, 2008.
- 19 Douglas, T. A., Fortier, D., Shur, Y. L., Kanevskiy, M. Z., Guo, L., Cai, Y., and Bray, M. T.:
20 Biogeochemical and geocryological characteristics of wedge and thermokarst-cave ice in
21 the CRREL permafrost tunnel, Alaska, *Permafrost and Periglacial Processes*, 22, 120-128,
22 doi:10.1002/ppp.709, 2011.
- 23 Finlay, J., Neff, J., Zimov, S., Davydova, A., and Davydov, S.: Snowmelt dominance of
24 dissolved organic carbon in high-latitude watersheds: Implications for characterization and
25 flux of river DOC, *Geophysical Research Letters*, 33, L10401,
26 doi:10.1029/2006GL025754, 2006.
- 27 Forbes, D. L.: State of the Arctic Coast 2010 – Scientific Review and Outlook, edited by:
28 International Arctic Science Committee (IASC), Land-Ocean Interactions in the Coastal
29 Zone (LOICS), Arctic Monitoring and Assessment Programme (AMAP), International
30 Permafrost Association (IPA), Helmholtz-Zentrum, Geesthacht, Geesthacht, 178, 2011.
- 31 French, H. M.: An appraisal of cryostratigraphy in north-west Arctic Canada, *Permafrost and*
32 *Periglacial Processes*, 9, 297-312, doi:10.1002/(SICI)1099-
33 1530(199810/12)9:4<297::AID-PPP296>3.0.CO;2-B, 1998.
- 34 Frey, K. E., and Smith, L. C.: Amplified carbon release from vast West Siberian peatlands by
35 2100, *Geophys. Res. Lett.*, 32, L09401, doi:10.1029/2004gl022025, 2005.
- 36 Fritz, M., Wetterich, S., Meyer, H., Schirrmeister, L., Lantuit, H., and Pollard, W. H.: Origin
37 and characteristics of massive ground ice on Herschel Island (western Canadian Arctic) as
38 revealed by stable water isotope and Hydrochemical signatures, *Permafrost and Periglacial*
39 *Processes*, 22, 26-38, doi:10.1002/ppp.714, 2011.
- 40 Fritz, M., Wetterich, S., Schirrmeister, L., Meyer, H., Lantuit, H., Preusser, F., and Pollard,
41 W. H.: Eastern Beringia and beyond: Late Wisconsinan and Holocene landscape dynamics

- 1 along the Yukon Coastal Plain, Canada, *Palaeogeography, Palaeoclimatology,*
2 *Palaeoecology*, 319–320, 28–45, doi:10.1016/j.palaeo.2011.12.015, 2012.
- 3 Gransee, A., and Führs, H.: Magnesium mobility in soils as a challenge for soil and plant
4 analysis, magnesium fertilization and root uptake under adverse growth conditions, *Plant*
5 *Soil*, 368, 5–21, doi:10.1007/s11104-012-1567-y, 2013.
- 6 Grosse, G., Robinson, J. E., Bryant, R., Taylor, M. D., Harper, W., DeMasi, A., Kyker-
7 Snowman, E., Veremeeva, A., Schirrmeister, L., and Harden, J.: Distribution of late
8 Pleistocene ice-rich syngenetic permafrost of the Yedoma Suite in east and central Siberia,
9 Russia, U.S. Geological Survey, Reston, Virginia, USA, 37, 2013.
- 10 Günther, F., Overduin, P. P., Sandakov, A. V., Grosse, G., and Grigoriev, M. N.: Short- and
11 long-term thermo-erosion of ice-rich permafrost coasts in the Laptev Sea region,
12 *Biogeosciences*, 10, 4297–4318, doi:10.5194/bg-10-4297-2013, 2013.
- 13 Günther, F., Overduin, P. P., Yakshina, I. A., Opel, T., Baranskaya, A. V., and Grigoriev, M.
14 N.: Observing Muostakh disappear: permafrost thaw subsidence and erosion of a ground-
15 ice-rich island in response to arctic summer warming and sea ice reduction, *The*
16 *Cryosphere*, 9, 151–178, doi:10.5194/tc-9-151-2015, 2015.
- 17 Guo, L., and Macdonald, R. W.: Source and transport of terrigenous organic matter in the
18 upper Yukon River: Evidence from isotope ($\delta^{13}\text{C}$, $\Delta^{14}\text{C}$, and $\delta^{15}\text{N}$) composition of
19 dissolved, colloidal, and particulate phases, *Global Biogeochemical Cycles*, 20, GB2011,
20 doi:10.1029/2005GB002593, 2006.
- 21 Guo, L., Ping, C.-L., and Macdonald, R. W.: Mobilization pathways of organic carbon from
22 permafrost to arctic rivers in a changing climate, *Geophysical Research Letters*, 34,
23 L13603, doi:10.1029/2007GL030689, 2007.
- 24 Harry, D. G., French, H. M., and Pollard, W. H.: Ice wedges and permafrost conditions near
25 King Point, Beaufort Sea coast, Yukon Territory, Paper 85-1A, Geological Survey of
26 Canada, Ottawa, 111–116, 1985.
- 27 Holmes, R., McClelland, J., Peterson, B., Tank, S., Bulygina, E., Eglinton, T., Gordeev, V.,
28 Gurtovaya, T., Raymond, P., Repeta, D., Staples, R., Striegl, R., Zhulidov, A., and Zimov,
29 S.: Seasonal and annual fluxes of nutrients and organic matter from large rivers to the
30 Arctic Ocean and surrounding seas, *Estuaries and Coasts*, 35, 369–382,
31 doi:10.1007/s12237-011-9386-6, 2012.
- 32 Horita, J., Ueda, A., Mizukami, K., and Takatori, I.: Automatic $[\delta]\text{D}$ and $[\delta]\text{18O}$
33 analyses of multi-water samples using H_2 - and CO_2 -water equilibration methods with a
34 common equilibration set-up, *International Journal of Radiation Applications and*
35 *Instrumentation. Part A. Applied Radiation and Isotopes*, 40, 801–805, doi:10.1016/0883-
36 2889(89)90100-7, 1989.
- 37 Hubberten, H.-W., Andreev, A., Astakhov, V. I., Demidov, I., Dowdeswell, J. A., Henriksen,
38 M., Hjort, C., Houmark-Nielsen, M., Jakobsson, M., Kuzmina, S., Larsen, E., Lunkka, J.
39 P., Lyså, A., Mangerud, J., Möller, P., Saarnisto, M., Schirrmeister, L., Sher, A. V.,
40 Siegert, C., Siegert, M. J., and Svendsen, J. I.: The periglacial climate and environment in
41 northern Eurasia during the Last Glaciation, *Quaternary Science Reviews*, 23, 1333–1357,
42 doi:10.1016/j.quascirev.2003.12.012, 2004.

- 1 Hugelius, G., Tarnocai, C., Broll, G., Canadell, J. G., Kuhry, P., and Swanson, D. K.: The
2 Northern Circumpolar Soil Carbon Database: spatially distributed datasets of soil coverage
3 and soil carbon storage in the northern permafrost regions, *Earth Syst. Sci. Data*, 5, 3-13,
4 doi:10.5194/essd-5-3-2013, 2013.
- 5 Hugelius, G., Strauss, J., Zubrzycki, S., Harden, J. W., Schuur, E. A. G., Ping, C. L.,
6 Schirrmeister, L., Grosse, G., Michaelson, G. J., Koven, C. D., O'Donnell, J. A., Elberling,
7 B., Mishra, U., Camill, P., Yu, Z., Palmtag, J., and Kuhry, P.: Improved estimates show
8 large circumpolar stocks of permafrost carbon while quantifying substantial uncertainty
9 ranges and identifying remaining data gaps, *Biogeosciences Discuss.*, 11, 4771-4822,
10 doi:10.5194/bgd-11-4771-2014, 2014.
- 11 Jolliffe, I. T.: *Principal Component Analysis*, 2nd Edn., Springer Series in Statistics, Springer,
12 New York, 488 pp., 2002.
- 13 Jorgenson, M. T., and Brown, J.: Classification of the Alaskan Beaufort Sea Coast and
14 estimation of carbon and sediment inputs from coastal erosion, *Geo-Marine Letters*, 25,
15 69-80, doi:10.1007/s00367-004-0188-8, 2005.
- 16 Kanevskiy, M., Shur, Y., Fortier, D., Jorgenson, M. T., and Stephani, E.: Cryostratigraphy of
17 late Pleistocene syngenetic permafrost (yedoma) in northern Alaska, Itkillik River
18 exposure, *Quaternary Research*, 75, 584-596, doi:10.1016/j.yqres.2010.12.003, 2011.
- 19 Kanevskiy, M., Shur, Y., Jorgenson, M. T., Ping, C. L., Michaelson, G. J., Fortier, D.,
20 Stephani, E., Dillon, M., and Tumskey, V.: Ground ice in the upper permafrost of the
21 Beaufort Sea coast of Alaska, *Cold Regions Science and Technology*, 85, 56-70,
22 doi:10.1016/j.coldregions.2012.08.002, 2013.
- 23 Kling, G. W., Kipphut, G. W., and Miller, M. C.: Arctic lakes and streams as gas conduits to
24 the atmosphere: implications for tundra carbon budgets, *Science*, 251, 298-301,
25 doi:10.1126/science.251.4991.298, 1991.
- 26 Kokelj, S. V., Smith, C. A. S., and Burn, C. R.: Physical and chemical characteristics of the
27 active layer and permafrost, Herschel Island, western Arctic Coast, Canada, *Permafrost
28 and Periglacial Processes*, 13, 171-185, doi:10.1002/ppp.417, 2002.
- 29 Lachniet, M. S., Lawson, D. E., and Sloat, A. R.: Revised ¹⁴C dating of ice wedge growth in
30 interior Alaska (USA) to MIS 2 reveals cold paleoclimate and carbon recycling in ancient
31 permafrost terrain, *Quaternary Research*, 78, 217-225, doi:10.1016/j.yqres.2012.05.007,
32 2012.
- 33 Lantuit, H., Rachold, V., Pollard, W. H., Steenhuisen, F., Ødegård, R., and Hubberten, H.-W.:
34 Towards a calculation of organic carbon release from erosion of Arctic coasts using non-
35 fractal coastline datasets, *Marine Geology*, 257, 1-10, doi:10.1016/j.margeo.2008.10.004,
36 2009.
- 37 Lantuit, H., Overduin, P., Couture, N., Wetterich, S., Aré, F., Atkinson, D., Brown, J.,
38 Cherkashov, G., Drozdov, D., Forbes, D., Graves-Gaylord, A., Grigoriev, M., Hubberten,
39 H.-W., Jordan, J., Jorgenson, T., Ødegård, R., Ogorodov, S., Pollard, W., Rachold, V.,
40 Sedenko, S., Solomon, S., Steenhuisen, F., Streletskaia, I., and Vasiliev, A.: The Arctic
41 Coastal Dynamics Database: A New Classification Scheme and Statistics on Arctic

- 1 Permafrost Coastlines, *Estuaries and Coasts*, 35, 383-400, doi:10.1007/s12237-010-9362-
2 6, 2012.
- 3 Lepš, J., and Šmilauer, P.: *Multivariate Analysis of Ecological Data using CANOCO*,
4 Cambridge University Press, 2003.
- 5 Mackay, J. R.: Glacier ice-thrust features of the Yukon Coast, *Geographical Bulletin*, 13, 5-
6 21, 1959.
- 7 McGuire, A. D., Anderson, L. G., Christensen, T. R., Dallimore, S., Guo, L., Hayes, D. J.,
8 Heimann, M., Lorenson, T. D., Macdonald, R. W., and Roulet, N.: Sensitivity of the
9 carbon cycle in the Arctic to climate change, *Ecological Monographs*, 79, 523-555,
10 doi:10.1890/08-2025.1, 2009.
- 11 Meyer, H., Schönicke, L., Wand, U., Hubberten, H. W., and Friedrichsen, H.: Isotope studies
12 of hydrogen and oxygen in ground ice – Experiences with the equilibration technique,
13 *Isotopes in Environmental and Health Studies*, 36, 133 - 149, 2000.
- 14 Meyer, H., Dereviagin, A., Siegert, C., Schirrmeister, L., and Hubberten, H.-W.: Paleoclimate
15 reconstruction on Big Lyakhovsky Island, north Siberia – hydrogen and oxygen isotopes in
16 ice wedges, *Permafrost and Periglacial Processes*, 13, 91-105, doi:10.1002/ppp.416, 2002.
- 17 Meyer, H., Yoshikawa, K., Schirrmeister, L., and Andreev, A.: The Vault Creek Tunnel
18 (Fairbanks region, Alaska) – A late Quaternary palaeoenvironmental permafrost record,
19 Ninth International Conference on Permafrost (NICOP), Fairbanks, Alaska, June 29 - July
20 3, 2008.
- 21 Meyer, H., Schirrmeister, L., Andreev, A., Wagner, D., Hubberten, H.-W., Yoshikawa, K.,
22 Bobrov, A., Wetterich, S., Opel, T., Kandiano, E., and Brown, J.: Lateglacial and Holocene
23 isotopic and environmental history of northern coastal Alaska – Results from a buried ice-
24 wedge system at Barrow, *Quaternary Science Reviews*, 29, 3720-3735,
25 doi:10.1016/j.quascirev.2010.08.005, 2010a.
- 26 Meyer, H., Schirrmeister, L., Yoshikawa, K., Opel, T., Wetterich, S., Hubberten, H.-W., and
27 Brown, J.: Permafrost evidence for severe winter cooling during the Younger Dryas in
28 northern Alaska, *Geophys. Res. Lett.*, 37, L03501, doi:10.1029/2009GL041013, 2010b.
- 29 Meyer, H., Opel, T., Laepple, T., Dereviagin, A. Y., Hoffmann, K., and Werner, M.: Long-
30 term winter warming trend in the Siberian Arctic during the mid- to late Holocene, *Nature*
31 *Geosci.*, 8, 122-125, 10.1038/ngeo2349, 2015.
- 32 Murton, J. B.: Stratigraphy and palaeoenvironments of Richards Island and the eastern
33 Beaufort Continental Shelf during the last glacial-interglacial cycle, *Permafrost and*
34 *Periglacial Processes*, 20, 107-125, doi:10.1002/ppp.647, 2009.
- 35 Nørgaard-Pedersen, N., Spielhagen, R. F., Erlenkeuser, H., Grootes, P. M., Heinemeier, J.,
36 and Knies, J.: Arctic Ocean during the Last Glacial Maximum: Atlantic and polar domains
37 of surface water mass distribution and ice cover, *Paleoceanography*, 18, 1063,
38 doi:10.1029/2002PA000781, 2003.
- 39 Olefeldt, D., and Roulet, N. T.: Effects of permafrost and hydrology on the composition and
40 transport of dissolved organic carbon in a subarctic peatland complex, *J. Geophys. Res.*,
41 117, G01005, doi:10.1029/2011jg001819, 2012.

- 1 Opel, T., Dereviagin, A. Y., Meyer, H., Schirrmeister, L., and Wetterich, S.: Palaeoclimatic
2 information from stable water isotopes of Holocene ice wedges on the Dmitrii Laptev
3 Strait, northeast Siberia, Russia, *Permafrost and Periglacial Processes*, 22, 84-100,
4 doi:10.1002/ppp.667, 2011.
- 5 Opsahl, S., and Benner, R.: Distribution and cycling of terrigenous dissolved organic matter
6 in the ocean, *Nature*, 386, 480-482, doi:10.1038/386480a0, 1997.
- 7 Ping, C.-L., Michaelson, G. J., Guo, L., Jorgenson, M. T., Kanevskiy, M., Shur, Y., Dou, F.,
8 and Liang, J.: Soil carbon and material fluxes across the eroding Alaska Beaufort Sea
9 coastline, *Journal of Geophysical Research: Biogeosciences*, 116, G02004,
10 doi:10.1029/2010JG001588, 2011.
- 11 Rachold, V., Eicken, H., Gordeev, V. V., Grigoriev, M. N., Hubberten, H. W., Lisitzin, A. P.,
12 Shevchenko, V. P., and Schirrmeister, L.: Modern Terrigenous Organic Carbon Input to
13 the Arctic Ocean, in: *The Organic Carbon Cycle in the Arctic Ocean*, edited by: Stein, R.,
14 and MacDonald, R., Springer Berlin Heidelberg, 33-55, 2004.
- 15 Rampton, V. N.: Quaternary geology of the Yukon Coastal Plain, *Geological Survey of
16 Canada Bulletin 317*, Geological Survey of Canada, Ottawa, 49p, 1982.
- 17 Raymond, P. A., McClelland, J. W., Holmes, R. M., Zhulidov, A. V., Mull, K., Peterson, B.
18 J., Striegl, R. G., Aiken, G. R., and Gurtovaya, T. Y.: Flux and age of dissolved organic
19 carbon exported to the Arctic Ocean: A carbon isotopic study of the five largest arctic
20 rivers, *Global Biogeochem. Cycles*, 21, GB4011, doi:10.1029/2007gb002934, 2007.
- 21 Schirrmeister, L., Grosse, G., Kunitsky, V., Magens, D., Meyer, H., Dereviagin, A.,
22 Kuznetsova, T., Andreev, A., Babiy, O., Kienast, F., Grigoriev, M., Overduin, P. P., and
23 Preusser, F.: Periglacial landscape evolution and environmental changes of Arctic lowland
24 areas for the last 60 000 years (western Laptev Sea coast, Cape Mamontov Klyk), *Polar
25 Research*, 27, 249-272, doi:10.1111/j.1751-8369.2008.00067.x, 2008.
- 26 Schirrmeister, L., Grosse, G., Schnelle, M., Fuchs, M., Krbetschek, M., Ulrich, M., Kunitsky,
27 V., Grigoriev, M., Andreev, A., Kienast, F., Meyer, H., Babiy, O., Klimova, I., Bobrov, A.,
28 Wetterich, S., and Schwamborn, G.: Late Quaternary paleoenvironmental records from the
29 western Lena Delta, Arctic Siberia, *Palaeogeography, Palaeoclimatology, Palaeoecology*,
30 299, 175-196, doi:10.1016/j.palaeo.2010.10.045, 2011a.
- 31 Schirrmeister, L., Grosse, G., Wetterich, S., Overduin, P. P., Strauss, J., Schuur, E. A. G., and
32 Hubberten, H.-W.: Fossil organic matter characteristics in permafrost deposits of the
33 northeast Siberian Arctic, *J. Geophys. Res.*, 116, G00M02, doi:10.1029/2011jg001647,
34 2011b.
- 35 Schirrmeister, L., Kunitsky, V., Grosse, G., Wetterich, S., Meyer, H., Schwamborn, G.,
36 Babiy, O., Dereviagin, A., and Siegert, C.: Sedimentary characteristics and origin of the
37 Late Pleistocene Ice Complex on north-east Siberian Arctic coastal lowlands and islands –
38 A review, *Quaternary International*, 241, 3-25, doi:10.1016/j.quaint.2010.04.004, 2011c.
- 39 Schirrmeister, L., Froese, D., Tumskey, V., and Wetterich, S.: Yedoma: Late Pleistocene Ice-
40 Rich Syngenetic Permafrost of Beringia, in: *The Encyclopedia of Quaternary Science*,
41 edited by: Elias, S. A., Elsevier, Amsterdam, 542-552, 2013.

- 1 Schneider von Deimling, T., Meinshausen, M., Levermann, A., Huber, V., Frieler, K.,
2 Lawrence, D. M., and Brovkin, V.: Estimating the near-surface permafrost-carbon
3 feedback on global warming, *Biogeosciences*, 9, 649-665, doi:10.5194/bg-9-649-2012,
4 2012.
- 5 Schuur, E. A. G., Vogel, J. G., Crummer, K. G., Lee, H., Sickman, J. O., and Osterkamp, T.
6 E.: The effect of permafrost thaw on old carbon release and net carbon exchange from
7 tundra, *Nature*, 459, 556-559, doi:10.1038/nature08031, 2009.
- 8 Schuur, E. A. G., and Abbott, B.: Climate change: High risk of permafrost thaw, *Nature*, 480,
9 32-33, doi:10.1038/480032a, 2011.
- 10 Schwamborn, G., Rachold, V., and Grigoriev, M. N.: Late Quaternary sedimentation history
11 of the Lena Delta, *Quaternary International*, 89, 119-134, doi:10.1016/s1040-
12 6182(01)00084-2, 2002.
- 13 Sellmann, P. V., and Brown, J.: Stratigraphy and diagenesis of perennially frozen sediments
14 in the Barrow, Alaska, region, 2nd International Conference on Permafrost, Yakutsk,
15 Russia, 13-28 July 1973, 1973, 171-181.
- 16 Shur, Y., French, H. M., Bray, M. T., and Anderson, D. A.: Syngenetic permafrost growth:
17 cryostratigraphic observations from the CRREL tunnel near Fairbanks, Alaska, *Permafrost*
18 *and Periglacial Processes*, 15, 339-347, doi:10.1002/ppp.486, 2004.
- 19 Strauss, J., Schirrmeister, L., Grosse, G., Wetterich, S., Ulrich, M., Herzsuh, U., and
20 Hubberten, H.-W.: The deep permafrost carbon pool of the Yedoma region in Siberia and
21 Alaska, *Geophys. Res. Lett.*, 40, GL058088, doi:10.1002/2013GL058088, 2013.
- 22 Striegl, R. G., Aiken, G. R., Dornblaser, M. M., Raymond, P. A., and Wickland, K. P.: A
23 decrease in discharge-normalized DOC export by the Yukon River during summer through
24 autumn, *Geophys. Res. Lett.*, 32, L21413, doi:10.1029/2005gl024413, 2005.
- 25 Tarnocai, C., Canadell, J. G., Schuur, E. A. G., Kuhry, P., Mazhitova, G., and Zimov, S.: Soil
26 organic carbon pools in the northern circumpolar permafrost region, *Global Biogeochem.*
27 *Cycles*, 23, GB2023, doi:10.1029/2008gb003327, 2009.
- 28 ter Braak, C. J. F., and Smilauer, P.: CANOCO reference manual and CanoDraw for
29 Windows user's guide : software for canonical community ordination (version 4.5),
30 Biometris, Wageningen [etc.], 2002.
- 31 Ulrich, M., Grosse, G., Strauss, J., and Schirrmeister, L.: Quantifying wedge-ice volumes in
32 Yedoma and thermokarst basin deposits, *Permafrost and Periglacial Processes*, 25, 151-
33 161, doi:10.1002/ppp.1810, 2014.
- 34 van Everdingen, R. O.: Multi-language glossary of permafrost and related ground-ice terms,
35 National Snow and Ice Data Center/World Data Center for Glaciology, Boulder, 1998.
- 36 Vonk, J. E., Sanchez-Garcia, L., van Dongen, B. E., Alling, V., Kosmach, D., Charhin, A.,
37 Semiletov, I. P., Dudarev, O. V., Shakhova, N., Roos, P., Eglinton, T. I., Andersson, A.,
38 and Gustafsson, O.: Activation of old carbon by erosion of coastal and subsea permafrost
39 in Arctic Siberia, *Nature*, 489, 137-140, doi:10.1038/nature11392, 2012.

- 1 Vonk, J. E., Mann, P. J., Davydov, S., Davydova, A., Spencer, R. G. M., Schade, J., Sobczak,
2 W. V., Zimov, N., Zimov, S., Bulygina, E., Eglinton, T. I., and Holmes, R. M.: High
3 biolability of ancient permafrost carbon upon thaw, *Geophysical Research Letters*, 40,
4 2689-2693, doi:10.1002/grl.50348, 2013a.
- 5 Vonk, J. E., Mann, P. J., Dowdy, K. L., Davydova, A., Davydov, S. P., Zimov, N., Spencer,
6 R. G. M., Bulygina, E. B., Eglinton, T. I., and Holmes, R. M.: Dissolved organic carbon
7 loss from Yedoma permafrost amplified by ice wedge thaw, *Environmental Research*
8 *Letters*, 8, 035023, doi:10.1088/1748-9326/8/3/035023, 2013b.
- 9 Walter Anthony, K. M., Zimov, S. A., Grosse, G., Jones, M. C., Anthony, P. M., Iii, F. S. C.,
10 Finlay, J. C., Mack, M. C., Davydov, S., Frenzel, P., and Frolking, S.: A shift of
11 thermokarst lakes from carbon sources to sinks during the Holocene epoch, *Nature*, 511,
12 452-456, doi:10.1038/nature13560, 2014.
- 13 Wegner, C., Bennett, K.E., de Vernal, A., Forwick, M., Fritz, M., Heikkilä, M., Łacka, M.,
14 Lantuit, H., Laska, M., Moskalik, M., O'Regan, M., Pawłowska, J., Promińska, A.,
15 Rachold V., Vonk, J.E., and Werner, K.: Variability in transport of terrigenous material on
16 the shelves and the deep Arctic Ocean during the Holocene, *Polar Res.*, in review.
- 17 Wetterich, S., Schirrmeister, L., Andreev, A. A., Pudenz, M., Plessen, B., Meyer, H., and
18 Kunitsky, V. V.: Eemian and Late Glacial/Holocene palaeoenvironmental records from
19 permafrost sequences at the Dmitry Laptev Strait (NE Siberia, Russia), *Palaeogeography,*
20 *Palaeoclimatology, Palaeoecology*, 279, 73-95, doi:10.1016/j.palaeo.2009.05.002, 2009.
- 21 Wetterich, S., Rudaya, N., Tumskey, V., Andreev, A. A., Opel, T., Schirrmeister, L., and
22 Meyer, H.: Last Glacial Maximum records in permafrost of the East Siberian Arctic,
23 *Quaternary Science Reviews*, 30, 3139-3151, doi:10.1016/j.quascirev.2011.07.020, 2011.
- 24 Wetterich, S., Tumskey, V., Rudaya, N., Andreev, A. A., Opel, T., Meyer, H., Schirrmeister,
25 L., and Hüls, M.: Ice Complex formation in arctic East Siberia during the MIS3
26 Interstadial, *Quaternary Science Reviews*, 84, 39-55, doi:10.1016/j.quascirev.2013.11.009,
27 2014.
- 28 Willerslev, E., Davison, J., Moora, M., Zobel, M., Coissac, E., Edwards, M. E., Lorenzen, E.
29 D., Vestergard, M., Gussarova, G., Haile, J., Craine, J., Gielly, L., Boessenkool, S., Epp, L.
30 S., Pearman, P. B., Cheddadi, R., Murray, D., Brathen, K. A., Yoccoz, N., Binney, H.,
31 Cruaud, C., Wincker, P., Goslar, T., Alsos, I. G., Bellemain, E., Brysting, A. K., Elven, R.,
32 Sonstebo, J. H., Murton, J., Sher, A., Rasmussen, M., Ronn, R., Mourier, T., Cooper, A.,
33 Austin, J., Moller, P., Froese, D., Zazula, G., Pompanon, F., Rioux, D., Niderkorn, V.,
34 Tikhonov, A., Savvinov, G., Roberts, R. G., MacPhee, R. D. E., Gilbert, M. T. P., Kjaer,
35 K. H., Orlando, L., Brochmann, C., and Taberlet, P.: Fifty thousand years of Arctic
36 vegetation and megafaunal diet, *Nature*, 506, 47-51, doi:10.1038/nature12921, 2014.
- 37 Zhang, T., Barry, R. G., Knowles, K., Heginbottom, J. A., and Brown, J.: Statistics and
38 characteristics of permafrost and ground-ice distribution in the Northern Hemisphere, *Polar*
39 *Geography*, 23, 132-154, doi:10.1080/10889379909377670, 1999.
- 40 Zimov, S. A., Davydov, S. P., Zimova, G. M., Davydova, A. I., Schuur, E. A. G., Dutta, K.,
41 and Chapin, F. S., III: Permafrost carbon: Stock and decomposability of a globally
42 significant carbon pool, *Geophys. Res. Lett.*, 33, L20502, doi:10.1029/2006gl027484,
43 2006a.

- 1 Zimov, S. A., Schuur, E. A. G., and Chapin, F. S.: Permafrost and the Global Carbon Budget,
- 2 Science, 312, 1612-1613, doi:10.1126/science.1128908, 2006b.
- 3 Zuur, A. F., Ieno, E. N., and Smith, G. M.: Analysing Ecological Data, Springer, New York,
- 4 2007.
- 5

6 **Tables**

7

8 **Table 1.** Summary of study areas, study sites, stratigraphy of the host sediments, ground-ice inventory and the studied ice types.

Region	Location	Longitude	Latitude	Stratigraphy and host sediments	Ground-ice conditions (inventory, ground-ice types, sampled ice types marked in <i>italic</i>)	Reference
Western Laptev Sea	Cape Mamontov Klyk	117.2	73.6	<ul style="list-style-type: none"> Fluvial bottom sands – Late Weichselian Ice Complex – Lateglacial to Holocene thermokarst deposits – Holocene valley deposits – Holocene cover deposits Yedoma hills (20-40 m a.s.l.) of ice-rich permafrost sequences with wide and deep syngenetic ice wedges separated by thermoerosional valleys and thermokarst depressions 	Ice-rich permafrost sequences with wide and deep syngenetic <i>late Pleistocene ice wedges</i>	Schirrmeister et al., 2008; Schirrmeister et al., 2011b; Boereboom et al., 2013
Lena Delta	Samoylov Island	126.4	72.4	<ul style="list-style-type: none"> First terrace (0-10 m a.s.l.): early to late Holocene delta floodplain, along the main river channels in the central and eastern parts of the delta; fluvial facies from organic-rich sands to silty-sandy peats towards bottom-up Modern to late Holocene floodplain; alluvial facies from peaty sands to silty-sandy peats bottom-up 	Ice-rich permafrost with active and buried syngenetic <i>Holocene ice wedges</i> Ice-rich permafrost with epigenetic <i>Holocene ice wedges</i>	Schwaborn et al., 2002; Schirrmeister et al., 2011a; Meyer et al., 2015
Eastern Laptev Sea	Muostakh Island	129.9	71.6	<ul style="list-style-type: none"> Lateglacial and Holocene cover deposits on top of Ice Complex Middle to Late Weichselian Ice Complex 	Very ice-rich permafrost, <i>late Pleistocene ice wedges, Holocene ice wedges</i>	Schirrmeister et al., 2011b, c (and references therein), Günther et al., 2015
Dmitry Laptev	Oyogos Yar coast	143.5	72.7	<ul style="list-style-type: none"> Alternation of wide thermokarst depressions (alases) and hills representing remnants of Ice-Complex deposits (Yedoma) 	Late Pleistocene and	Wetterich et al., 2009;

Strait				<ul style="list-style-type: none"> • Lateglacial to Holocene thermokarst deposits and on top of Ice Complex • Taberite formed during Weichselian to Holocene transition • Late Weichselian Ice Complex • Middle Weichselian Ice Complex 	<p><i>Holocene ice wedges,</i></p> <p>All ice wedges were sampled at a coastal bluff at an elevation of about 10 m a.s.l. in a central alas depression</p>	<p>Opel et al., 2011; Schirrmeister et al., 2011b</p>
New Siberian Islands	Bol'shoy Lyakhovsky Island	143.9	73.2	<ul style="list-style-type: none"> • Late Holocene cover deposits and Holocene valley deposits • Lateglacial to Holocene thermokarst deposits • Taberite formed during Weichselian to Holocene transition • Middle Weichselian Ice Complex 	<p><i>Late Pleistocene ice wedges</i></p>	<p>Meyer et al., 2002 ; Andreev et al., 2004, 2009; Schirrmeister et al., 2011b; Wetterich et al., 2011, 2014</p>
Northern Alaska	Barrow (CRREL Permafrost Tunnel)	-156.7	71.3	Buried ice-wedge system under about three meters of Lateglacial to early Holocene ice-rich sediments	<p><i>Lateglacial ice wedges,</i> Holocene ice wedges</p>	<p>Sellman and Brown, 1973; Meyer et al., 2010a, b</p>
Interior Alaska	Fairbanks (Vault Creek Tunnel)	-147.7	65.0	Discontinuous permafrost. Late Pleistocene ice-rich silty, loess-like organic-rich sediments between 12-15 m thick with large intersecting ice wedges	<p><i>Late Pleistocene ice wedges,</i> Holocene ice wedges</p>	<p>Shur, et al. 2004; Meyer et al., 2008</p>
Yukon Coast	Komakuk Beach	-140.5	69.6	<ul style="list-style-type: none"> • Middle and late Holocene ice-rich peat, polygonal tundra • Early Holocene thaw-lake sediments, peat, ice wedge casts • Late Wisconsin (i.e. Late Weichselian) proluvial, alluvial, eolian deposits 	<p>Holocene ice wedges, <i>Holocene snow pack ice (fossil snow bank)</i></p>	<p>Rampton, 1982; Fritz et al., 2012</p>
Yukon Coast	Herschel Island	-139.1	69.6	<ul style="list-style-type: none"> • Retrogressive thaw slumps along the coast exposing massive ground ice and ice-rich sediments 	<p><i>Buried glacier ice</i> of \geq 20 m thickness within</p>	<p>Mackay, 1959; Rampton,</p>

				<ul style="list-style-type: none"> • Holocene cover deposits and slope material along steep coastal bluffs • Mixed origin of marine, near-shore and terrestrial deposits • Push end-moraine of Late Wisconsin age 	<p>Late Wisconsin diamicton</p> <p><i>Late Wisconsin ice wedges</i> truncated by mass movement and early Holocene thaw unconformity</p> <p>Epigenetic and anti-syngenetic <i>Holocene ice wedges</i></p> <p><i>Buried lake ice</i>, fossil snow bank ice</p>	<p>1982; Fritz et al., 2011, 2012</p>
Yukon Coast	Roland Bay	-139.0	69.4	<ul style="list-style-type: none"> • Retrogressive thaw slumps along the coast exposing massive ground ice and ice-rich sediments • Holocene cover deposits and slope material along steep coastal bluffs • Late Wisconsin diamicton 	<p><i>Late Wisconsin and Holocene ice wedges</i></p>	<p>Rampton, 1982</p>
Yukon Coast	Kay Point	-138.2	69.2	<ul style="list-style-type: none"> • Retrogressive thaw slumps along the coast exposing massive ground ice and ice-rich sediments • Holocene cover deposits and slope material along steep coastal bluffs • Moraine (ridge) of Late Wisconsin age 	<p>Presumably <i>Late Wisconsin buried glacier ice, Holocene ice wedges</i></p>	<p>Rampton, 1982; Harry et al., 1985</p>

1 [Table 2](#). Summarized DOC and DIC concentrations of different massive ground-ice types. For
 2 individual sample values see [Supplement Table S1](#).

Ice type	DOC			DIC			No. of ice bodies	No. of samples	Stratigraphic affiliation
	DOC Mean [mg L ⁻¹]	DOC concentration range [mg L ⁻¹]	No. of ice bodies	No. of samples	DIC Mean [mg L ⁻¹]	DIC concentration range [mg L ⁻¹]			
Ice wedge ice	9.6	1.6–28.6	22	72	4.7	0.3–19.8	21	66	Holocene, Late Pleistocene
Basal glacier ice	1.8	0.7–3.8	5	22	9.3	0.1–25.4	4	19	Late Pleistocene
Buried lake ice	2.0	0.3–5.2	1	6	8.8	0.3–22.9	1	6	Late Pleistocene
Snow pack ice	3.0	n.a.	1	1	n.a.	n.a.	0	0	Holocene
<i>Modern surface water</i>	5.6	5.5–5.7	3	3	22.6	5.0–40.2	3	3	<i>recent</i>

3 Three modern surface water samples are from three different water bodies representing thermokarst
 4 ponds along the Yukon Coast.

5
 6

1 **Table 3.** DOC stocks and pools in late Pleistocene and Holocene permafrost containing ice
 2 wedges (IW) based on calculated wedge-ice volumes (WIV) in Yedoma and thermokarst
 3 basin deposits. All other ground-ice types, especially non-massive intrasedimental ice, are not
 4 included.

	DOC concentrati on in Pleistocen e IW mg L ⁻¹	DOC concentrati on in Holocene IW mg L ⁻¹	WIV in Pleistoce ne Yedoma deposits vol%	WIV in Holocene thermoka rst deposits vol%	DOC stocks in Pleistoce ne permafro st ^c g m ⁻³	DOC stocks in Holocen e permafr ost ^c g m ⁻³	DOC pools in Pleistoce ne permafro st ^{c, d} Tg	DOC pools in Holocen e permafr ost ^{c, d} Tg
Min	2.4	1.6	16.7 ^a	1.0 ^a	0.4	0.02	3.2	0.07
Mea n	11.1	7.3	48.0 ^b	7.0 ^b	5.3	0.51	43.0	2.2
Max	28.6	19.5	63.2 ^a	13.2 ^a	18.1	2.6	145.9	11.0

5 ^a WIV data by [Ulrich et al., 2014](#). ^b Mean WIV data by [Strauss et al., 2013](#). ^c This includes ice wedges
 6 only. ^d According to [Strauss et al. \(2013\)](#) undisturbed Pleistocene Yedoma covers 416,000 km² with a
 7 mean thickness of 19.4 m, whereas Holocene thermokarst deposits cover 775,000 km² with a mean
 8 thickness of 5.5 m.

9
 10

1 **Figures**

2

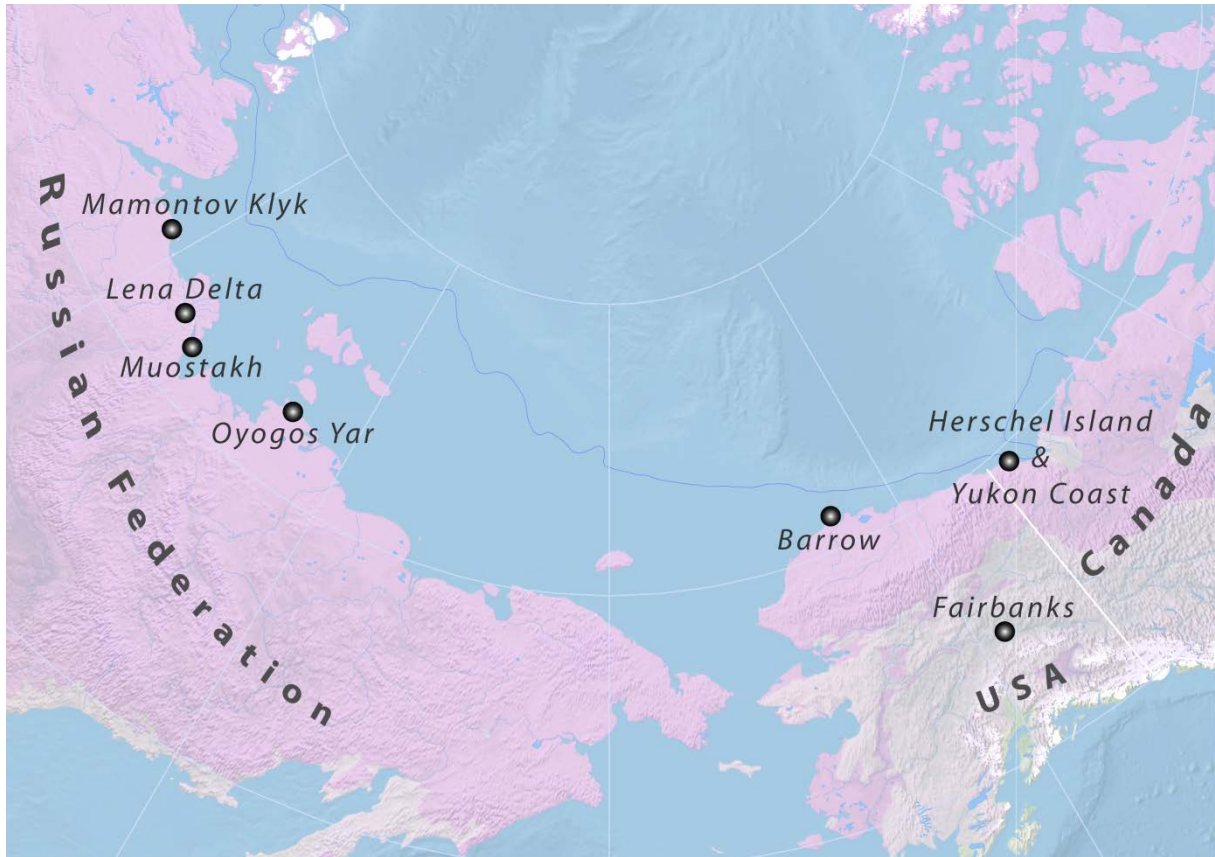


Figure 1. Study area and study sites (dots) for massive ground ice sampling in the Arctic lowlands of Siberia and North America. All study sites are located within the zone of continuous permafrost (dark purple), except for the Fairbanks area, which is the zone of discontinuous permafrost (light purple). Blue line in the Arctic Ocean marks the northerly extent of submarine permafrost according to [Brown et al. \(1997\)](#).

3

4



Ice-rich late Pleistocene permafrost, Oyogos Yar, Russia



Ice-rich permafrost coast, Muostakh, Russia



Epigenetic Holocene ice wedge, Lena Delta (Samoylov Island), Russia



Syngenetic late Pleistocene ice wedge, Mamontov Klyk, Russia



Buried glacier ice, Herschel Island, Canada



Snow pack ice, Herschel Island, Canada



Buried lake ice, Herschel Island, Canada

Figure 2. Ground-ice conditions and examples of studied ground-ice types in the Siberian and North American Arctic. Place names are plotted on Fig. 1.

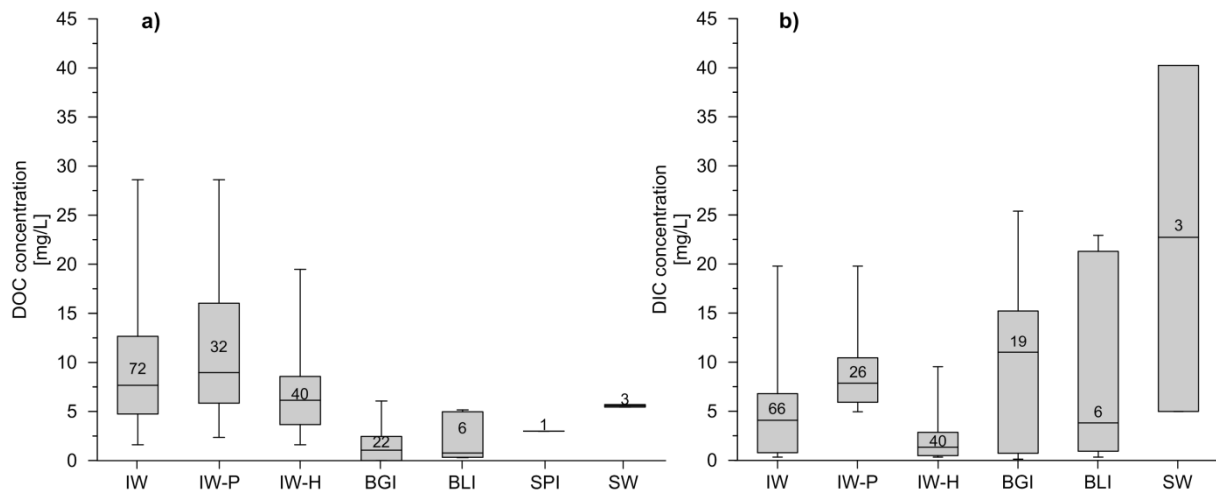


Figure 3. Boxplots of (a) DOC and (b) DIC concentrations in different massive ground-ice types. Plots show the number of samples in each category, minimum, maximum, median, 25 per cent-quartile and 75 per cent quartile as edge of boxes. IW: Ice wedges (all), IW-P: Pleistocene ice wedges, IW-H: Holocene ice wedges, BGI: Buried glacier ice, BLI: Buried lake ice, SPI: Snow pack ice, SW: Surface water. For individual sample values see [Supplement Table S1](#).

1

2

DOC – unsorted correlation matrix

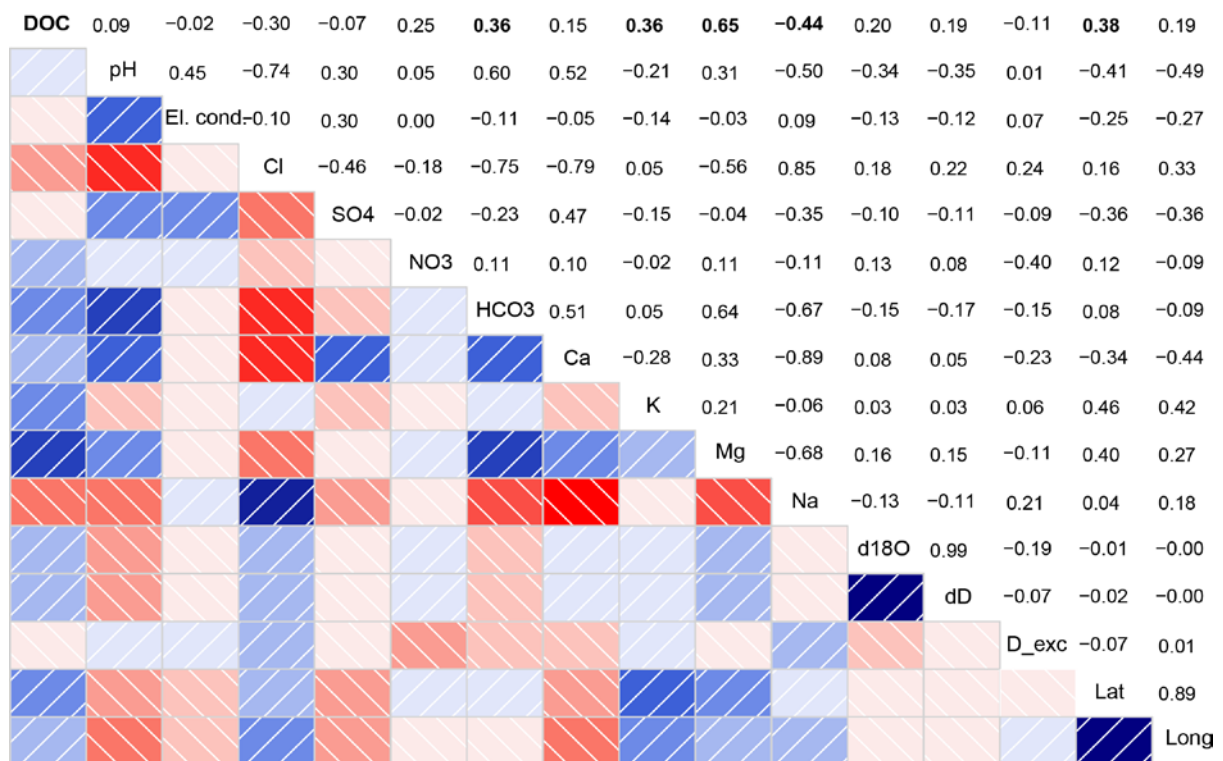


Figure 4. Correlation matrix. Correlations mentioned in the text are printed in bold. Strong positive correlations of paired variables are indicated by dark bluish colors, while strong anti-correlations are depicted in red. Hatching from the upper right to the lower left depict positive correlations, whereas negative correlations are reversely hatched for better perceptibility in a black-and-white print. (For interpretation of the references to color in this figure legend, the reader is referred to the web version of this article.)

1

2

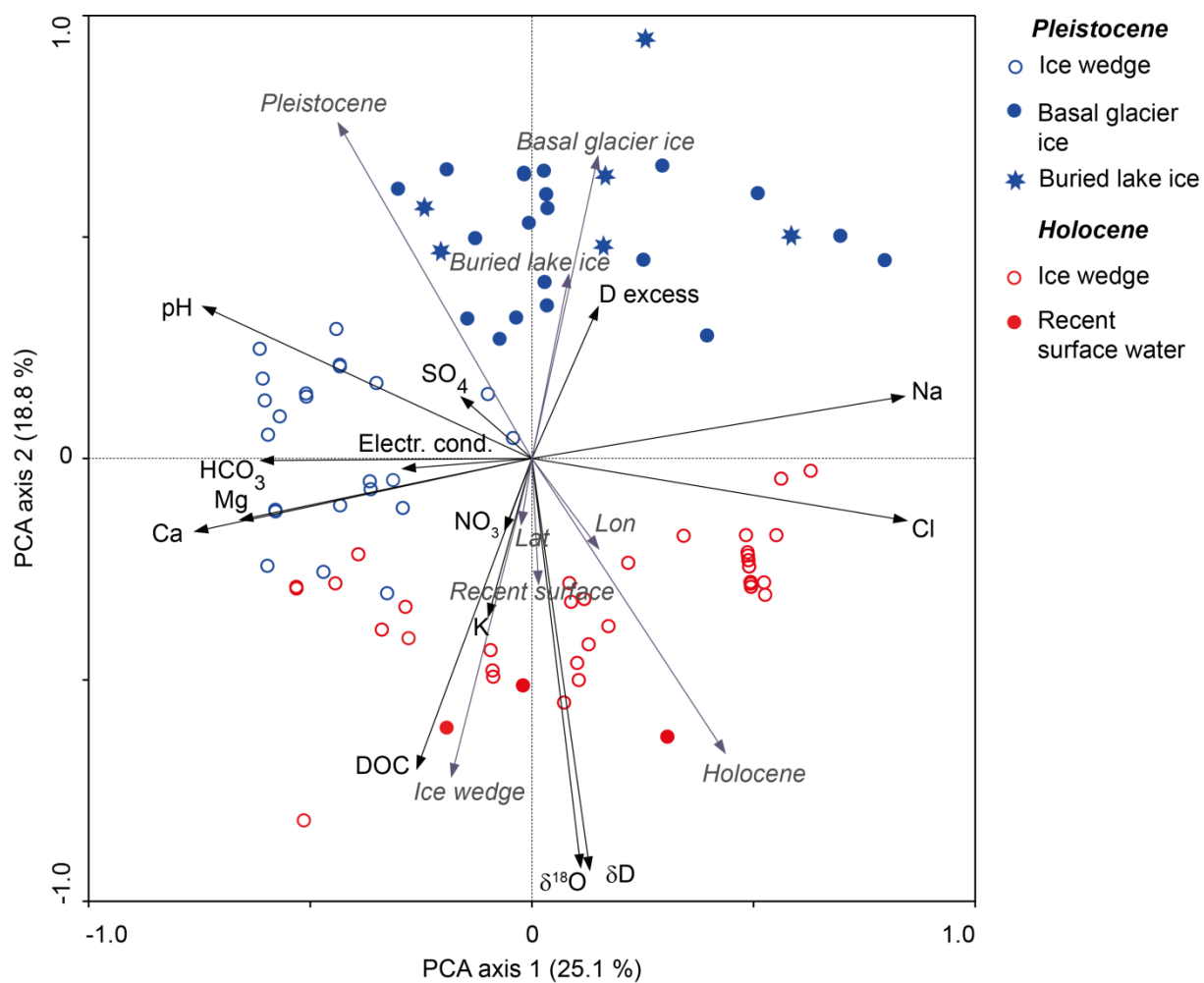


Figure 5. PCA biplot for ground-ice data. Inactive supplementary parameters (i.e. ice wedge, buried lake ice, basal glacier ice, snow pack ice, surface water, Pleistocene, Holocene, recent) are shown in grey italic. For individual sample values see [Supplement Table S1](#).

1

2

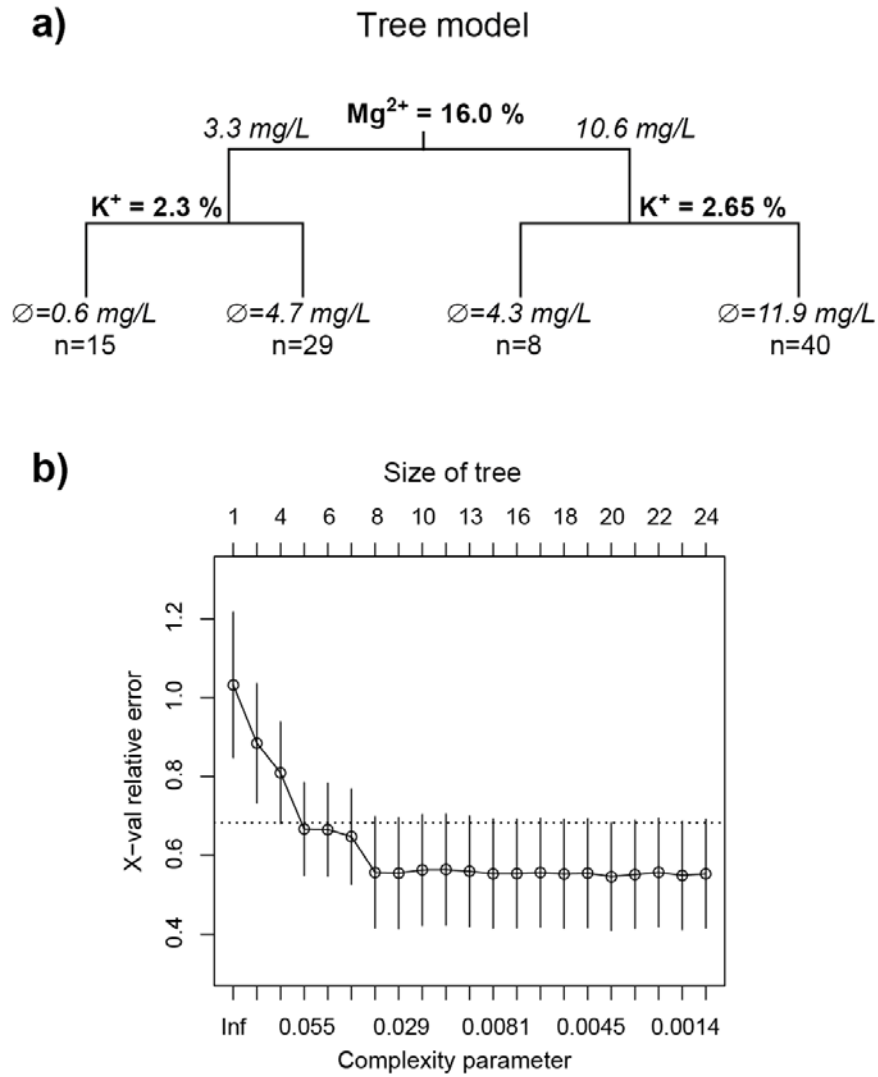


Figure 6. Univariate Tree Model (UTM) explains variability pattern in DOC concentration. a) Tree model focuses on DOC concentration as response variable. UTM uses 92 observations and a set of 22 explanatory variables. Mg^{2+} and K^+ ions are most important to explain differences in DOC concentrations. Mean DOC concentrations of each group in $mg L^{-1}$. Number of observations in each group (n). b) Cross validation determines the statistically significant size of the tree model. The dotted line is obtained by the mean value of the errors (x-error) of the cross validations plus the standard deviation of the cross validations upon convergence. For individual sample values see [Supplement Table S1](#).